Assessment of Usability of WC-Co Powder Mixtures for SLM

David Bricin, Antonin Kriz
Department of Material Science and Technology, Faculty of Mechanical Engineering, University of West Bohemia, Univerzitni 8, 301 00, Pilsen. Czech Republic. bricda@kmm.zcu.cz, kriz@kmm.zcu.cz

This paper aims to provide comprehensive information on the usability of WC-Co powder mixtures for the additive technology of selective laser melting (SLM). Three different WC-Co powder mixtures and a precipitation-hardenable steel powder, which is ordinarily used for this process, were compared. Metallographic analysis by means of optical and scanning electron microscopes was performed for evaluating their properties. Phase composition of the powders was studied using X-ray analysis. Results of these analyses enable the WC-Co powder mixtures to be ranked in the order of suitability for the SLM process.

Keywords: SLM Technology, WC-Co Powders, Particle Shape, Particle Distribution, Particle Size

1 Introduction

The primary use of WC-Co powder mixtures is the manufacture of products of simple shapes. These include exchangeable cutting inserts, drill heads, axial cutting tools and parts of basic shapes for applications where high hardness is demanded whereas toughness less so. Powder mixtures are shaped by isostatic pressing, extrusion of injection moulding. [1] Using these processes, only basic shapes can be produced without any intricate cavities for lightweighting or cooling of the part. However, intricate parts are increasingly made using additive technologies. It involves creating the final product layer by layer from powder, filament or pellets. [2] Thanks to the stepwise nature of the process, extraordinary structures can be built with fewer structural details, such as weld or screw joints. Consequently, the costs of production can be reduced, along with the repair costs.

The ordinary materials for additive manufacturing include polymers, non-ferrous metals and steels. [2]

This experimental study deals with the usability of WC-Co powders for the additive technology SLM. As described above, these powder mixtures are not used for additive manufacturing in industrial practice. Some companies, however, have already begun exploring this field, which was the motivation for this study. In addition, the author of this study focuses on this matter in his doctoral thesis.

1.1 Requirements for powder mixtures for SLM

Powder mixtures which are to be used for SLM should conform to certain specifications. If these are met and the process settings are correct, low-porosity products can be obtained with the desired uniform mechanical and physical properties. Fundamental requirements for powder mixtures include:

-Uniform chemical composition of powder particles. If the chemical composition of particles were varied, the melting temperature, weldability and mechanical properties would be inhomogeneous. [3]

-Certain distribution of powder particle sizes. This depends on the method used, such as SLM/SLS, EBM or LMD. Most additive manufacturing machines, including those based on SLM, accept powders with particle sizes of 10-50 μm. Smaller particles are undesirable, as they have a negative impact on fluidity of the mixture. The distribution of particle sizes plays a role in the fluidity of powder, its ability to spread over the build platform, the density of the powder layer, the surface roughness of the build and on the amount of energy required for melting. [3]

-Morphology and rheological properties. Particles should be spherical and free of surface defects, such as craters, cavities and satellites, i.e. joints between larger and smaller particles. Such defects impair the fluidity, uniformity and density of a powder layer. [3–4]

In addition, powder mixtures should contain as little residual moisture as possible. Consequently, they should be stored in an appropriate protective atmosphere or in the presence of silica gel desiccant. The reason is that at higher moisture levels, pores form during sintering, which is part of the additive manufacturing process. [3]

Hence, powder mixtures must possess two fundamental properties. The first is good fluidity. [5] The second is adequate apparent density. Powders which exhibit an appropriate combination of these properties can form a uniform layer for trouble-free sintering on the build platform. [3–4]

2 Experimental methods

2.1 Specification of experiments

The experiments consisted of metallographic examination of powder mixtures using a Carl Zeiss ObserverZ1m optical microscope and a PHILIPS XL30 ESEM scanning electron microscope, a chemical composition analysis of powder particles using EDX, and a phase composition analysis by X-ray diffraction. Statistical evaluation of the data from metallographic examination was performed using the NIS Elements and Axio Vision software tools. The metallographic examination consisted of two stages. In the first stage, the surface, size and shape of powder particles, as well as their surface defects were studied. In the second stage, metallographic sections through the particles were prepared. Using these sections, the distribution of phases within the particles was examined. Various etching techniques were employed to reveal the microstructure of powder particles. Chemical etching

with Adler's reagent was used for the steel powder. Carbide-based powder mixtures were etched with reference to ASTM B 665 standard, which deals with preparation of metallographic specimens of cemented carbides and identification of phases in them. [6] The microstructures of WC-Co powder mixtures were revealed using chemical etching with Murakami's reagent combined with aqueous solution of hydrochloric acid.

2.2 Materials under analysis

Four powder mixtures were examined. Powder A was a precipitation-hardenable steel powder. It was employed as a reference specimen because it is ordinarily used for the SLM process. The other powder mixtures were commercially available WC-Co powders. Their properties are given below. The differences in their properties were due to differences in their production methods. [7] The powder mixtures are denoted as powders B, C and D. Table 1 gives their basic data.

Tab. 1 *Basic data on powder mixtures under analysis; chemical composition was measured using EDX*

Designation	Chemical composition					Applications
A	Cr	Ni	Cu	Si	Fe	SLS process
	13.7±0.4	4.0±0.2	3.6±0.15	0.5±0.1	balance	
B	WC	Co	O	Cr		HIP process
	76.0±2.8	16.0±1.3	7.0±1.5	0.3±0.3		
C	77.0±1.7	16.0±1.4	7.0±1.4	-		Thermally sprayed coatings
D	81±1	13.0±0.6	6.0±1.5	-		Binder jetting process

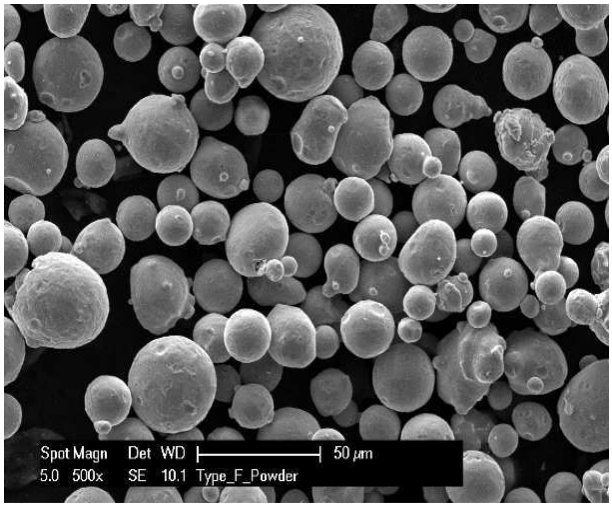

Fig. 1 *Particles of powder mixture A – reference specimen, magnification 500×*

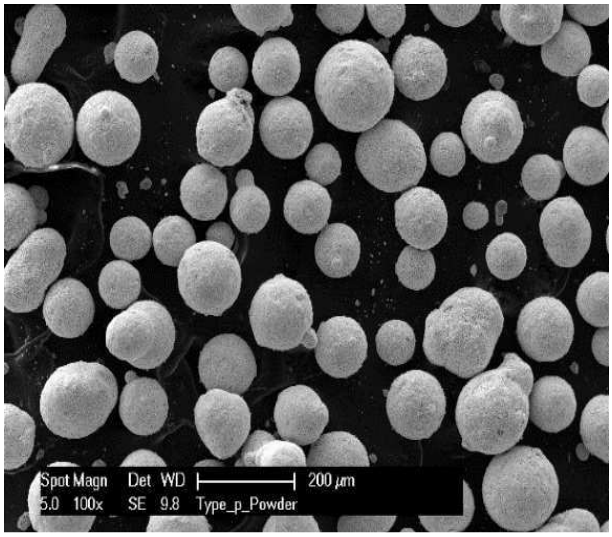

Fig. 2 *Particles of powder mixture B, magnification 100×*

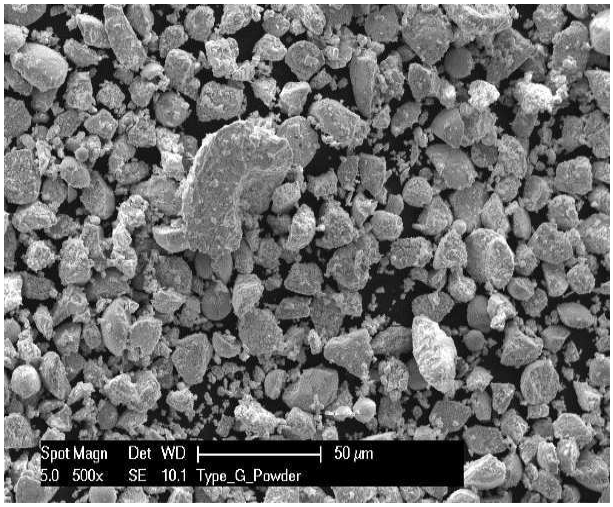

Fig. 3 *Particles of powder mixture C, magnification 500×*

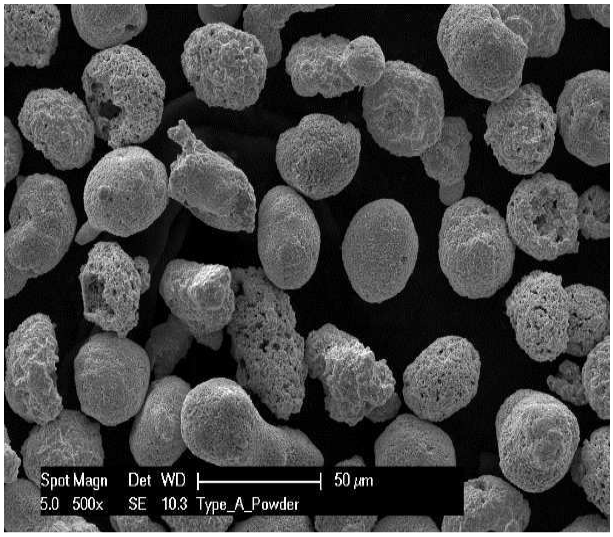

Fig. 4 *Particles of powder mixture D, magnification 500×*

3 Results and discussion

3.1 Analysis of powder particle surfaces

Micrographs in Figures 1–4 suggest that the powders were produced using different processes. Particles of the reference powder have smooth surfaces without pores or similar defects, Fig. 1. Particles of powder mixture D look different. Their surface contains craters and cavities, as seen in Fig. 4. Another distinction consists in the particle shape. In powder mixture C in Fig. 3, the particle shape is very different from the other powders. Small particles under 5 µm were detected in powder mixture C. They were found on the surface of larger WC-Co pellets, to which they adhered thanks to Van der Waals forces. [8] As mentioned in the introduction, such fine grains may impair the fluidity of a powder and prevent it from spreading appropriately across the build platform in the additive manufacturing equipment. Besides, they may be inhaled by the operator or escape through the machine's filtering system. Satellites, i.e. small particles attached to larger ones, formed in powder mixtures A and D. Their joints are the result of partial sintering during production. [1] The above micrographs clearly show that powder mixtures A and D were produced by atomization in inert gas or plasma. Powder mixture C is the result of atomization in water. Powder mixture B was obtained by joining WC and Co particles with an organic binder during milling and mixing in an attritor mill. [9] As a result, the surface of the powder particles appears to be smooth and defect-free, Fig. 2.

Compliance with the requirement for more or less consistent chemical composition of powder particles was checked using EDX. The phase composition of particles should be identical among and within the particles. Regions with different phases can be highlighted using BSE imaging, as shown in Figs. 5–8. In these images, the reference powder particles exhibit no variation in chemical composition, which suggests that they contain a single phase. In micrographs of the WC-Co powder mixtures, one can study the distribution of Co (dark regions) and WC (bright regions) phases in Figs. 6–8. This contrast is a result of different atomic numbers of the elements. It is therefore readily apparent that the distribution of the Co binder among WC grains is more uniform in powder mixtures C and D than in B.

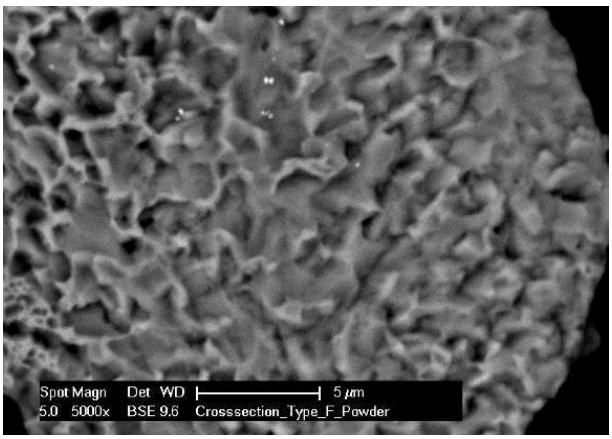

Fig. 5 *BSE image of the phase composition of a particle of the reference powder A, magnification 500×*

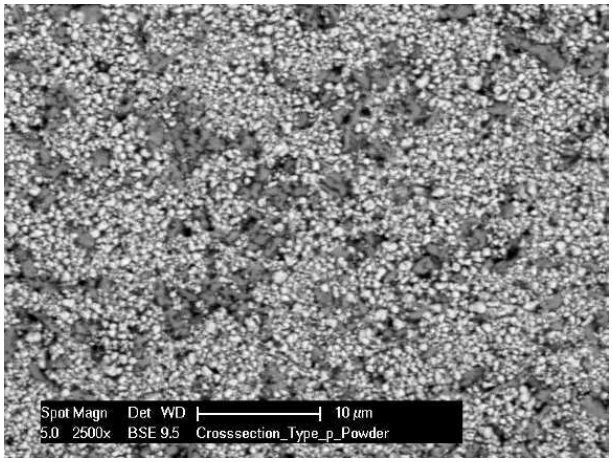

Fig. 6 *BSE image of the phase composition of a powder B particle, magnification 2500×*

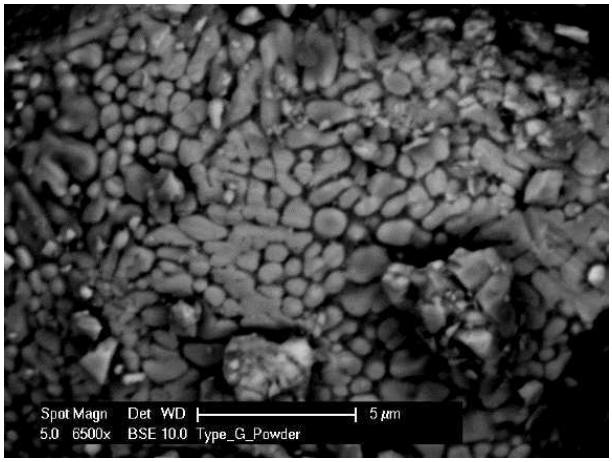

Fig. 7 *BSE image of the phase composition of a powder C particle, magnification 6500×*

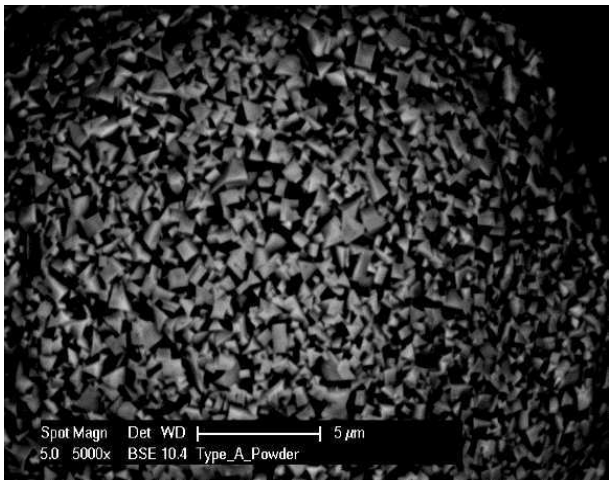

Fig. 8 *BSE image of the phase composition of a powder D particle, magnification 5000×*

The uniform chemical and structural composition of particles of the reference powder A is reflected in their complete melting upon interaction with the laser beam. By contrast, the particles of WC-Co powder mixtures fail to melt completely, and therefore sinter while partly solid. [2] This has a profound impact on porosity and mechanical properties of the product.

3.2 Shape and size distribution of powder particles

The usability of a powder mixture for SLM strongly depends, among other aspects, on the size and shape of its particles. As mentioned in the introduction, it is important for the SLM equipment that the particles have a size between 10 and 50 μm and their shape is, preferably, spherical. Plots obtained from an analysis of sizes and shapes of particles of the test powders are shown in Figs. 9–10.

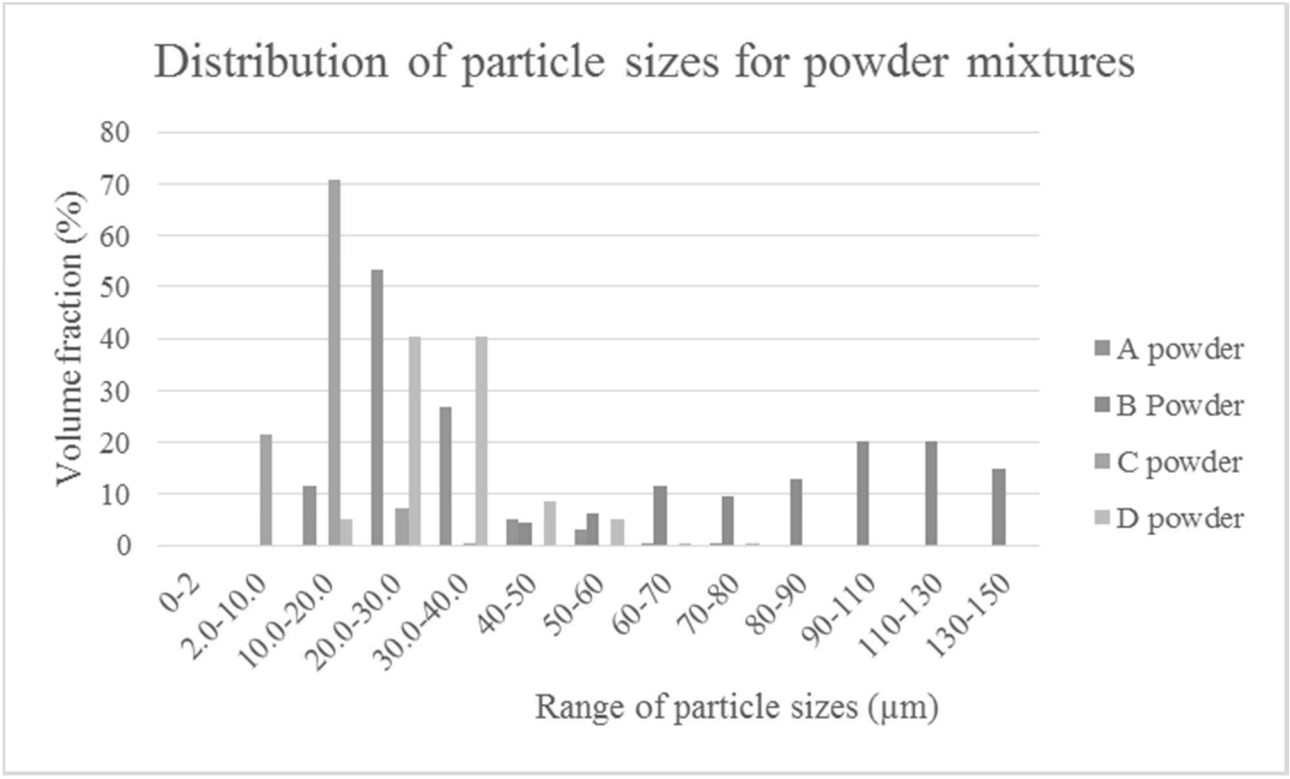

Fig. 9 *Powder particle sizes*

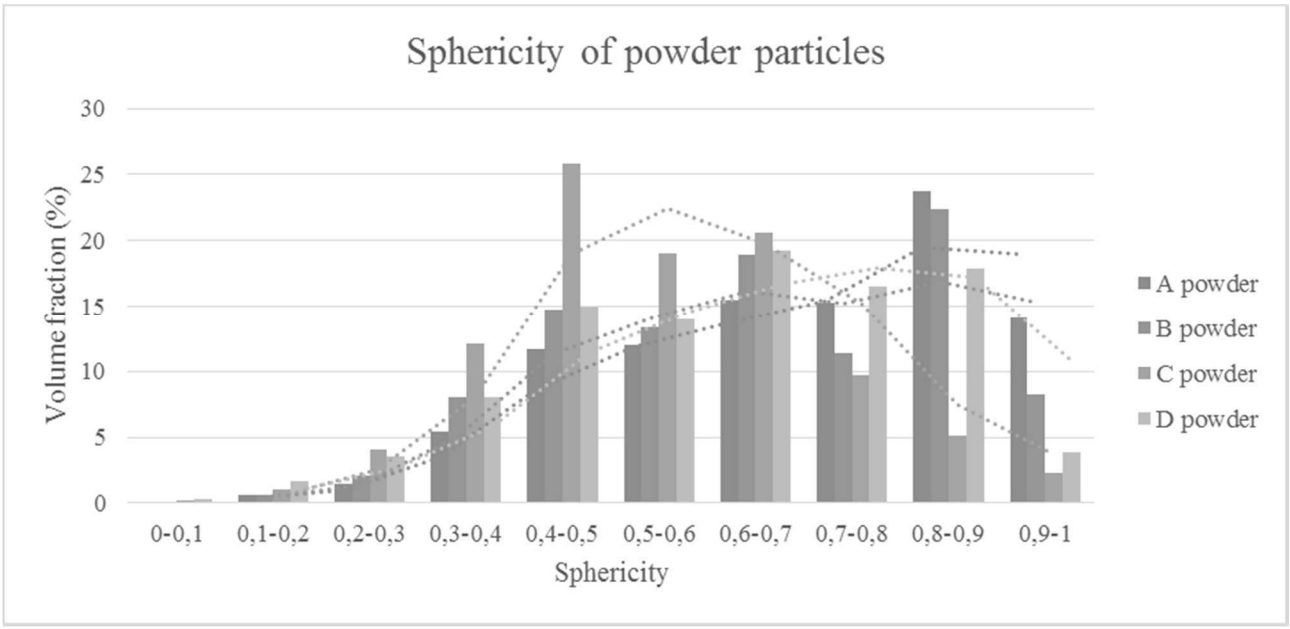

Fig. 10 *Powder particle shape. Unity denotes perfectly circular particles.*

The data in Fig. 9 suggests that the reference powder mixture A and powder mixture D meet the size limit for applicability. Powder mixture C contains a large fraction of fine particles which precludes its use in SLM equipment. Powder mixture B is non-conforming because of a large fraction of particles which are coarser than the upper limit for this additive technology. Nevertheless, it is likely to be usable in EBM or LMD equipment, thanks to its particle size distribution. [3]

Particles of the reference powder A and those of

powders B and D are closest to the ideal spherical shape. This was apparent from the micrographs in Figs. 1–4. The profiles of their shapes are very similar, as seen in the plot in Fig. 10. The plot also shows that most particles of powder mixture C are sharp-edged rather than spherical.

From these two analyses, one can derive that the lowest fluidity will be found in powder mixture C, owing to the undesirable particle shape and a large fraction of fine particles. Powder mixtures A and D, with their smallest variation in particle size and their particle shapes closest to a sphere, will possess the highest fluidity. In powder mixture B, the variation in particle size is much larger, resulting in larger contact areas between particles. Those slow down the particle flow and reduce fluidity.

3.3 Phase composition of particles

The reference steel powder was proven to contain a single phase. Observation of particle surfaces in WC-Co powder mixtures using BSE imaging revealed at least two phases: α-phase of a tungsten carbide and β-phase of the Co binder. In addition to those, cemented carbides may contain a γ-phase formed by cubic carbides, such as VC, TiC or TaC [1] or η-phase which consists of mixed tungsten and binder-based carbides.

The above phases were identified on transverse metallographic sections. After preparation, the metallographic sections were etched according to ASTM B657-92 to reveal their microstructure, as seen in Fig. 11–19. Chemical composition analysis by EDX found only WC tungsten carbide and Co binder in powder mixtures C and D. It is therefore unlikely that these specimens contain the above-named cubic carbides. This hypothesis was confirmed by etching for revealing this phase, as shown in Figs. 15 and 18. In powder mixture B, the EDX analysis found chromium which, in the form of carbides, inhibits the WC grain growth during sintering. It was impossible to directly prove the presence of γ-phase, as the etchant that was used for powder mixture B interacted with the organic binder. As a consequence, the microstructure became obscured, as seen in Figs. 11–13. Besides, identification of this phase was hampered by the size of WC grains and Co binder areas, which was around one micrometre, near the resolving power of the optical microscope used.

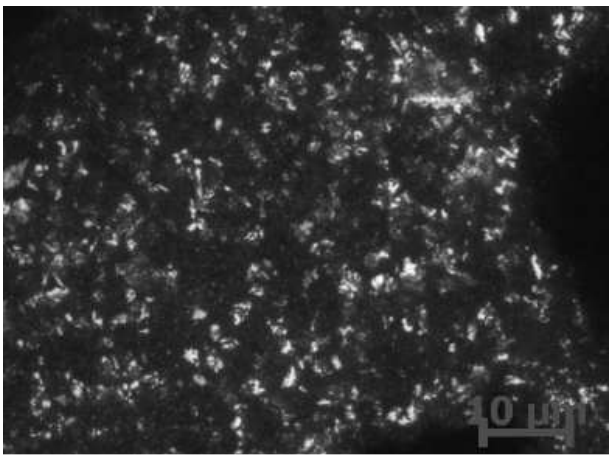

Fig. 11 *Powder mixture B, detection of alpha phase, etched with Murakami's reagent (5 minutes), magnification 1000×*

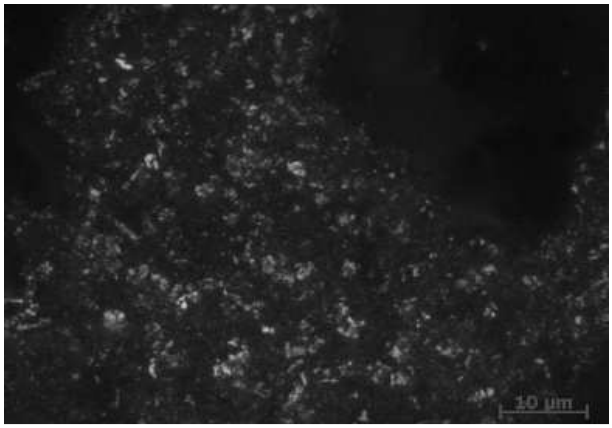

Fig. 12 *Powder mixture B, detection of gamma phase, etched with Murakami's reagent/aqueous solution of HCl/Murakami's reagent (3 min/10 s/20 s), magnification 1000×*

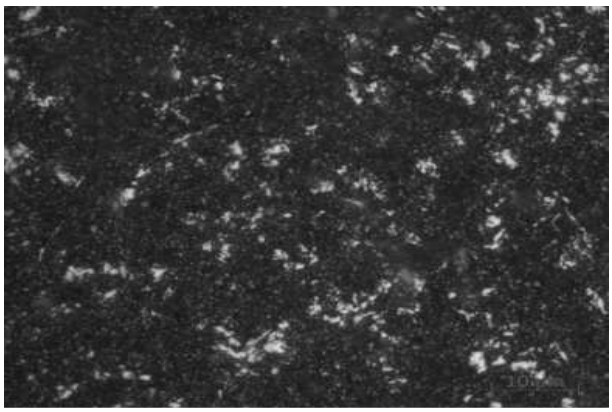

Fig. 13 *Powder mixture B, detection of eta phase, etched with Murakami's reagent (5 seconds), magnification 1000×*

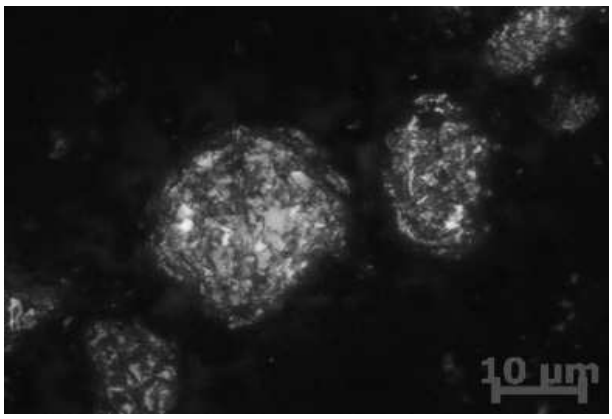

Fig. 14 *Powder mixture C, detection of alpha phase, etched with Murakami's reagent (5 minutes), magnification 1000×*

Etching for η-phase revealed its presence in powder mixture C, see Fig. 16, unlike in B and D. Depending on the particle size, this phase was either present throughout the particle or near its surface, Fig. 16. Whether this phase forms depends on the carbon distribution within the particle and on the cooling rate of the particle. It is more likely to develop at faster cooling rates. [1; 10] Its presence is evidence that the powder mixture was indeed made by

atomization in water. As a result, heat was rapidly removed from the particle surface, resulting in steep temperature gradients that promoted formation of this phase. The centres of particles, close to WC grains, cooled more uniformly and slowly, which is why the Co binder was preserved there.

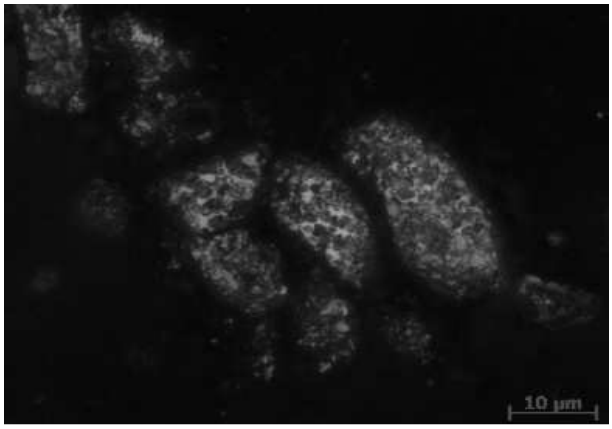

Fig. 15 *Powder mixture C, detection of gamma phase, etched with Murakami's reagent/aqueous solution of HCl/Murakami's reagent (3 min/10 s/20 s), magnification 1000×*

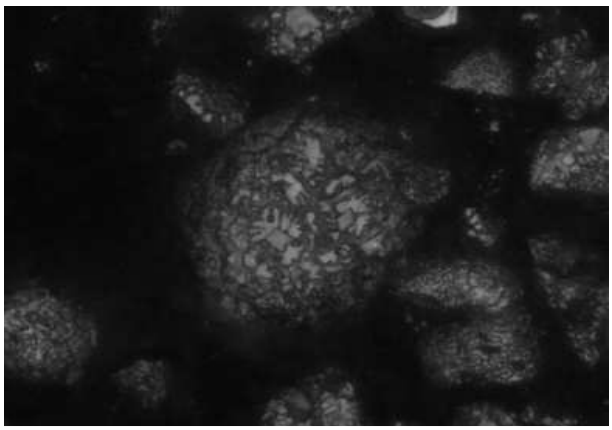

Fig. 16 *Powder mixture C, detection of eta phase, etched with Murakami's reagent (5 s), magnification 1000×*

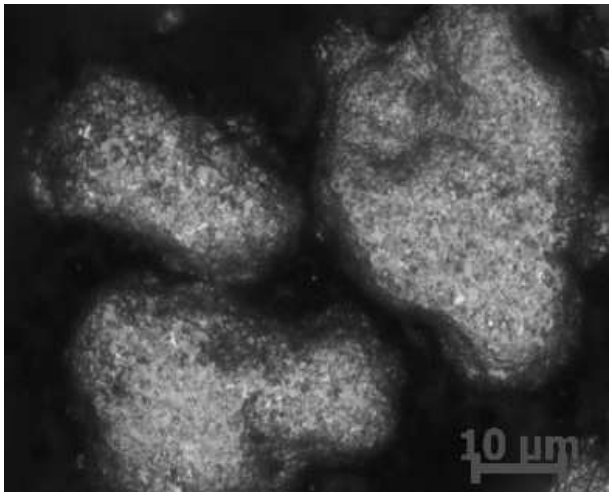

Fig. 17 *Powder mixture D, detection of alpha phase, etched with Murakami's reagent (5 min), magnification 1000×*

Colour etching revealed alpha and beta phases in powder mixture D, Figs. 17–19. Neither gamma nor eta phases were detected in this powder upon etching. Eta phase has not formed in this powder mixture because the particles were atomized in an inert gas, in which heat dissipation was slower than in water, leading to less favourable conditions for the phase to form.

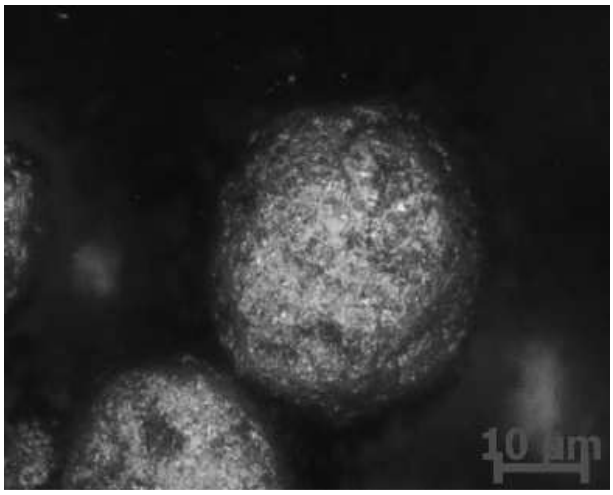

Fig. 18 *Powder mixture D, detection of gamma phase, etched with Murakami's reagent/aqueous solution of HCl/Murakami's reagent (3 min/10 s/20 s), magnification 1000×*

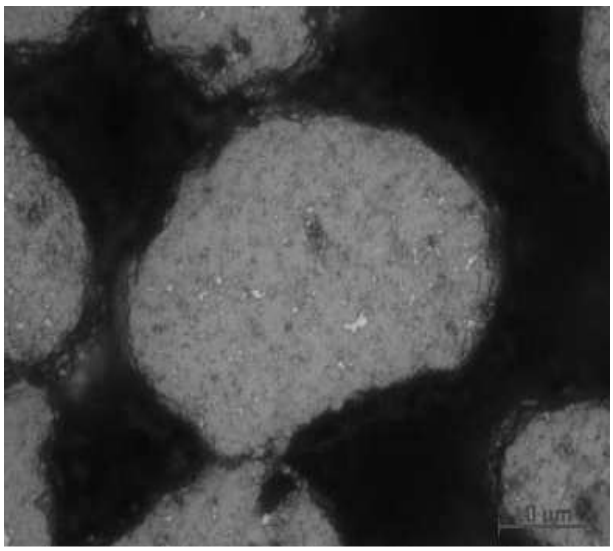

Fig. 19 *Powder mixture D, detection of eta phase, etched with Murakami's reagent (5 s), magnification 1000×*

The presence of the phases identified by metallographic analysis was confirmed by an X-ray diffraction analysis of the phase composition, as seen in Fig. 20 below.

In powder mixtures B–D, this analysis confirmed the presence of α-phase WC and β-phase Co. In powder mixture C, the W_2C phase, η-phase Co_3W_3C and the intermetallic $W_{0.2}Co_{0.8}$ were identified, in addition to the two phases mentioned. The last-named phase was also detected in powder mixture D.

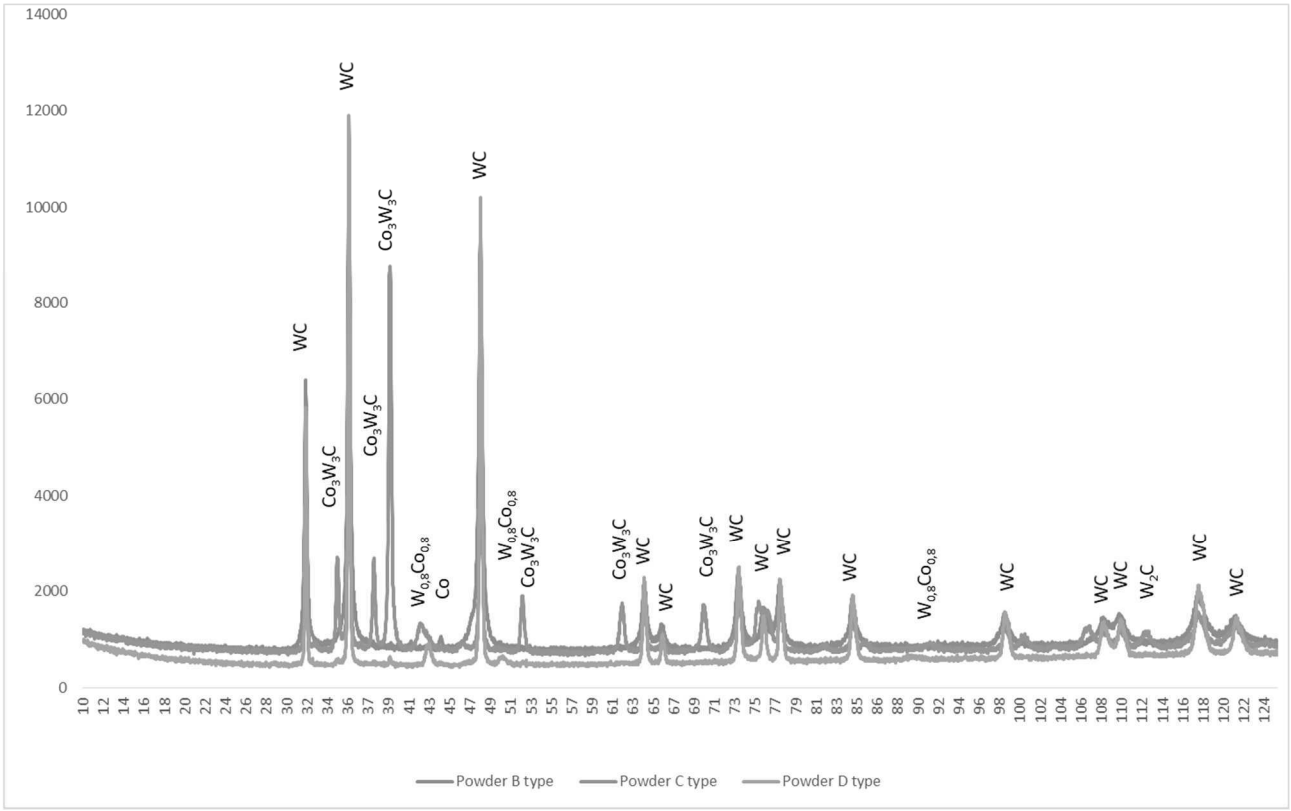

Fig. 20 *Phase compositions of powder mixtures B–D recorded using the X-ray diffraction method.*

4 Conclusion

This experimental study leads to the following conclusions regarding the usability of these WC-Co powder mixtures for SLM:

- WC-Co powder mixtures always contain no fewer than two phases: α and β. Besides them, powder mixture C was found by metallographic analysis to contain η-phase and $W_{0.2}Co_{0.8}$ intermetallic, where the latter was also confirmed by X-ray diffraction analysis to be present in powder mixture D. In addition to these, WC-Co powder mixtures may contain an organic binder, as found in powder mixture B. The presence of these phases causes non-uniform chemical composition within the interior of particles. As a result, the melting temperature and, in turn, the energy required for melting, varies within particles, which makes sintering difficult. This poses a major difference to the reference material A whose phase and chemical compositions are uniform, as are the melting temperatures of its particles and the energy required for melting. For this reason, WC-Co powders are not very suitable for the SLM process.
- In addition to phase composition, powder mixtures should meet specifications for particle size variation and rheological properties, i.e. the particle shape and surface defects. These analyses have shown that the particle shapes in powder mixtures B and D meed the requirements for use in the SLM process. Powder mixture C contains sharp-edged particles of non-uniform shapes and unfavourable sizes which impair fluidity. In terms of the variation in particle size, only powder mixture D met the specification for this application.

It follows from the above summary that, among the WC-Co mixtures under examination, the powder mixture which is most suitable for the SLM process is powder D. It has met the highest number of requirements which had been derived by comparing WC-Co powder mixtures and the reference powder mixture A.

Published findings were used as a basis for developing a follow-up experimental programme for modifying selected WC-Co powder mixtures and using them for the SLM additive technology.

Acknowledgement

Experimental research conducted in this study was supported under a project sponsored by the Technology Agency of the Czech Republic as part of the ZETA programme, no. TJ01000218, entitled "Manufacture of carbide cutting tool prototype by SLM additive manufacturing technique"

References

[1] EDITOR-IN-CHIEF VINOD K. SARIN a Luis LLanes EDITED BY DANIELE MARI. (2014). *Comprehensive hard materials*, Volume 1, Hard-metals. ISBN 9780080965284. Elsevier Publisher, Oxford.

[2] VENUVINOD, P. and MA, W. (2010). *Rapid prototyping*. Kluwer Academic. Boston.

[3] *EUROPEAN POWDER METALLURGY ASSOCIATION. (2017).* Introduction to Additive Manufacturing Technology*, 2nd Edition Revised (Web Only) 2017. Available from:* https://www.epma.com/epma-free-publications/product/introduction-to-additive-manufacturing-brochure

[4] SAMES, W. J., LIST,F. A., PANNALA, S., DEHOFF, R. R., AND BABU S. S. (2016). The metallurgy and processing science of metal additive manufacturing, International Materials Reviews

[5] POPOVICH, A., SUFIIAROV, V. (2018). *Metal Powder Additive Manufacturing*. DOI: 10.5772/63337. ISBN 978-953-51-2479-5. *Available from*: http://www.intechopen.com/books/new-trends-in-3d-printing/metal-powder-additive-manufacturing

[6] ASTM B657-92(1996)e1, *Standard Test Method for Metallographic Determination of Microstructure in Cemented Tungsten Carbides*, ASTM International, West Conshohocken, PA, 2000.

[7] DAWES, J., BOWERMAN, R., TREPLETON, R. (2015). Introduction to the Additive Manufacturing Powder Metallurgy Supply Chain. Johnson Matthey Technology. DOI: 10.1595/205651315X688686. ISSN 20565135. *Available from*: http://openurl.ingenta.com/content/xref?genre=article&issn=2056-5135&volume=59&issue=3&spage=243

[8] BRICÍN, D., ŠPIRIT, Z., KŘÍŽ, A. (2018). Metallographic Analysis of the Suitability of a WC-Co Powder Blend for Selective Laser Melting Technology. *Materials Science Forum*. DOI: 10.4028/www.scientific.net/MSF.919.3. ISSN 1662-9752. *Available from*: https://www.scientific.net/MSF.919.3

[9] NEIKOV, O., NABOYCHENKO, s. (2008). *Handbook of non-ferrous metal powders: technologies and applications*. ISBN 9781856174220. Elsevier .New York.

[10] HUMÁR, A. *Materials for cutting tools*. (2008). ISBN 978-80-254-2250-2. MM Publishing Prague.

[11] KUČEROVÁ, L., ZETKOVÁ, I. (2016). Metallography of 3D printed 1.2709 Tool Steel. (2016). *Manufacturing Technology,* volume 16. ISSN 1213-2489.

[12] FOUSOVÁ, M., VOJTĚCH, D., FOJT, J. (2016). Microscopic Evaluation of 3D-Printed Materials Surface and Characteristic Microstructure. (2016). *Manufacturing Technology,* volume 16. ISSN 1213-2489.

[13] FOUSOVÁ, M., VOJTĚCH, D., KUBÁSEK, J., DVORSKÝ, D., MACHOVÁ, M. (2015). 3D Printing as an Alternative to Casting Forging and Machining Technologies. (2015). *Manufacturing Technology*, volume 15. ISSN 1213-2489.

10.21062/ujep/166.2018/a/1213-2489/MT/18/5/719